

Hybrid Molecular Materials Based upon the Photochromic Nitroprusside Complex, [Fe(CN)₅NO]²⁻, and Organic π -Electron Donors. Synthesis, Structure, and Properties of the Radical Salt (TTF)₇[Fe(CN)₅NO]₂ (TTF = Tetrathiafulvalene)

M. Clemente-León,[†] E. Coronado,^{*,‡}
J. R. Galán-Mascarós,^{†,§} C. J. Gómez-García,[†] and
E. Canadell[§]

Instituto de Ciencia Molecular, Universitat de Valencia, Dr. Moliner 50, E-46100 Burjassot, Spain, and Institut de Ciència de Materials de Barcelona (CSIC), Campus de la UAB, 08193 Bellaterra, Spain

Received March 7, 2000

Introduction

Radical cation salts based on planar π -electron donors of the TTF type have received much attention as they provide many examples of molecular conductors and superconductors.¹ Typically they are formed by segregated stacks of the cation radicals interleaved with charge-compensating inorganic anions such as Cl⁻, Br⁻, I₃⁻, PF₆⁻, ClO₄⁻, BF₄⁻, etc. One of the current developments in this area is that of using as counterions metal complexes possessing "active" electrons (delocalized frontier orbitals, localized magnetic moments, etc.). This hybrid association can result in novel lattice architectures for the organic component and/or novel molecular materials with a combination of properties. Most of the efforts in this context focus on the design of materials combining conducting and magnetic properties,^{2–6} although other associations are also suitable. An attractive possibility is that of using the nitroprusside anion, [Fe(CN)₅NO]²⁻, which is interesting from the photophysical point of view because it exhibits a photoinduced transition to an extremely long-lived metastable state upon irradiation with light in the wavelength range 350–580 nm at temperatures below ca. 160 K.⁷ As this electronic transition is accompanied

Table 1. Crystal Data for (TTF)₇[Fe(CN)₅NO]₂

empirical formula	S ₂₈ C ₅₂ H ₂₈ Fe ₂ N ₁₂ O ₂	fw	1862.4
<i>a</i> , Å	10.536(2)	space group	P2 ₁ /c
<i>b</i> , Å	13.038(6)	ρ_{calcd} , g·cm ⁻³	1.708
<i>c</i> , Å	26.405(4)	λ , Å	0.710 69
β , deg	93.616(14)	μ , cm ⁻¹	12.59
<i>V</i> , Å ³	3620.0(19)	<i>R</i> ^a	0.0406
<i>Z</i>	4	<i>R</i> _w ^b	0.0910

^a $R = \sum ||F_o - F_c| / \sum |F_o|$. ^b $R_w = [\sum w(F_o^2 - F_c^2)^2 / \sum w(F_o^2)^2]^{1/2}$; $w = 1/[\sigma^2(F_o^2) + (0.0359P)^2 + 3.3459P]$, where $P = (F_o^2 + 2F_c^2)/3$.

by a possible change in the geometry of the complex, such a feature may affect the conductive properties of the radical salt. The nitroprusside salts so far investigated contain electronically "innocent" cations such as alkali-metal, alkaline-earth-metal, or tetraalkylammonium cations. The only example of association of the nitroprusside anion with TTF-type radicals was recently reported by Yu and Zhu.⁸ These authors prepared a bis-(ethylenedithio)tetrathiafulvalene (BEDT–TTF) salt that exhibited superconductivity at 7 K, although a more detailed study has indicated that this observation was probably an artifact.⁹ In this paper, we report the first radical salt formed by the organic π -electron donor TTF and the photochromic complex [Fe(CN)₅NO]²⁻. A preliminary account of this compound has already been communicated.¹⁰

Experimental Section

Synthesis. Shiny black prismatic crystals of the title compound were obtained after 2 weeks by electrochemical oxidation under low constant current ($I = 0.6 \mu\text{A}$) of a 1:4 benzonitrile/acetonitrile solution of neutral TTF (10^{-3} M) in the presence of the sodium salt of the nitroprusside anion (3×10^{-2} M) and dibenzo-18-crown-6 (4×10^{-2} M). The solvents were not previously dried. In fact, the addition of a few drops of water was necessary to obtain good-quality single crystals.

X-ray Crystal Structure Analysis. The crystals were mounted on an Enraf-Nonius CAD4 diffractometer. Unit cell parameters and the orientation matrix were determined by a standard least-squares refinement (Enraf-Nonius CAD4 software) of the setting angles of 25 automatically centered reflections. Data collection was performed by the ω - 2θ scan technique in a zigzag mode, and numerical data corrections were applied for Lorentz, polarization, and absorption effects (ψ scan). Selected experimental parameters and crystal data are reported in Table 1. All calculations were performed on a SPARC 20 station (Sun Microsystems). The structure was solved by direct methods using the SIR92¹¹ program, followed by a Fourier synthesis, and refined using the SHELXL-93 program (G. M. Sheldrick, University of Göttingen, 1993). All atoms except hydrogen and carbon atoms belonging to the TTF fragments were refined anisotropically.

Physical Measurements. Variable-temperature susceptibility measurements were carried out in the temperature range 2–300 K at a magnetic field of 0.1 T on polycrystalline samples by using a magnetometer (Quantum Design MPMS-XL-5) equipped with a SQUID sensor. The susceptibility data were corrected for the diamagnetism of the compound as deduced from Pascal's constant tables. Variable-temperature EPR spectra were recorded at X-band frequency on a

* Corresponding author. E-mail: eugenio.coronado@uv.es.

[†] Universitat de Valencia.

[‡] Present address: Department of Chemistry, Texas A&M University, College Station, TX 22843.

[§] Institut de Ciència de Materials de Barcelona.

- (1) Williams, J. M.; Ferraro, J. R.; Thorn, R. J.; Carlson, K. D.; Geiser, U.; Wang, H. H.; Kini, A. M.; Whangbo, M. H. In *Organic Superconductors (Including Fullerenes). Synthesis, Structure, Properties and Theory*; Grimes, R. N., Ed.; Prentice Hall: Englewood Cliffs, NJ, 1992.
- (2) Kurmoo, M.; Graham, A. W.; Day, P.; Coles, S. J.; Hursthouse, M. B.; Caulfield, J. L.; Singleton, J.; Pratt, F. L.; Hayes, W.; Ducasse, L.; Guionneau, P. *J. Am. Chem. Soc.* **1995**, *117*, 12209.
- (3) Almeida, M.; Gama, V.; Henriques, R. T.; Alcácer, L. In *Inorganic and Organometallic Polymers with Special Properties*; Laine, R. M., Ed.; Kluwer: Dordrecht, The Netherlands, 1992; p 163.
- (4) Kumai, R.; Asamitsu, A.; Tokura, Y. *Chem. Lett.* **1996**, 753.
- (5) Kobayashi, H.; Tomita, H.; Naito, T.; Kobayashi, A.; Sakai, F.; Watanabe, T.; Cassoux, P. *J. Am. Chem. Soc.* **1996**, *118*, 368.
- (6) (a) Coronado, E.; Falvello, L. R.; Galán-Mascarós, J. R.; Giménez-Saiz, C.; Gómez-García, C. J.; Lauhin, V. N.; Pérez-Benítez, A.; Rovira, C.; Veciana, J. *Adv. Mater.* **1997**, *9*, 984. (b) Coronado, E.; Gómez-García, C. J. *Chem. Rev.* **1998**, *98*, 273.
- (7) (a) Hauser, U.; Oestreich, V.; Rohrweck, H. D. *Z. Phys.* **1977**, *17*, A280. (b) Woike, Th.; Krasser, W.; Bechthold, P. S.; Haussühl, S. *Phys. Rev. Lett.* **1984**, *53*, 1767. (c) Carducci, M. D.; Fomitchev, D. V.; Coppens, P. *J. Am. Chem. Soc.* **1997**, *119*, 2669.

(8) Yu, H.; Zhu, D. *Physica C* **1997**, *282*, 1893.

- (9) (a) Kushch, L.; Buratov, L.; Tkacheva, V.; Yagubskii, E.; Zorina, L.; Khasanov, S.; Shibaeva, R. *Synth. Met.* **1999**, *102*, 1646 (Proceedings of the ICSM'98). (b) Gener, M.; Canadell, E.; Kashanov, S. S.; Zorina, L. V.; Shibaeva, R. P.; Kushch, L. A.; Yagubskii, E. B. *Solid State Commun.* **1999**, *111*, 329.
- (10) Clemente-León, M.; Coronado, E.; Galán-Mascarós, J. R.; Giménez-Saiz, C.; Gómez-García, C. J.; Fabre, J. M. *Synth. Met.* **1999**, *103*, 2279 (Proceedings of the ICSM'98).
- (11) Altomare, A.; Cascarano, G.; Giacovazzo, C.; Guagliardi, A. *J. Appl. Crystallogr.* **1994**, *27*, 1045.

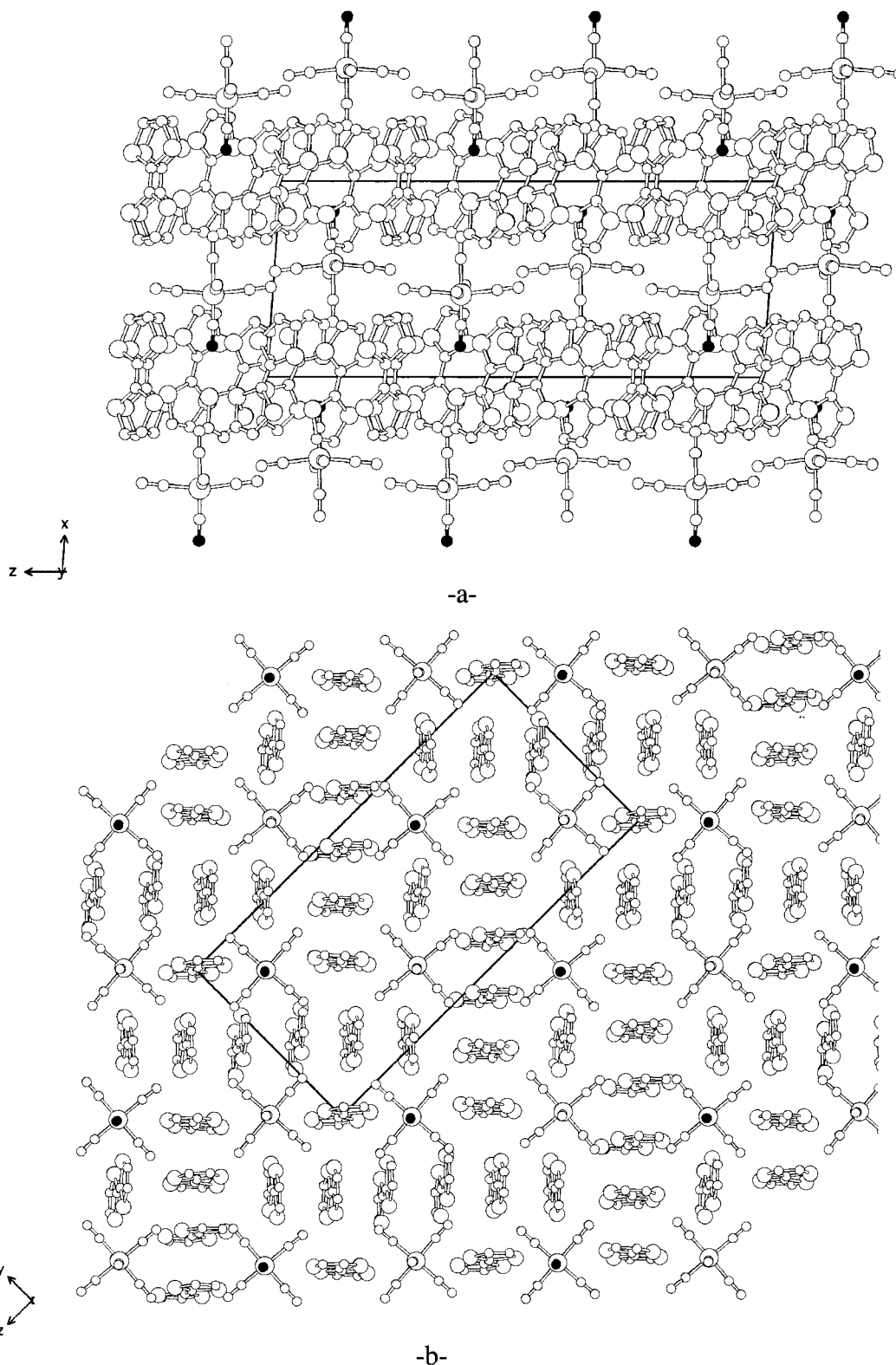


Figure 1. (a) View of the structure in the ac plane showing the alternating layers of TTF and nitroprusside with the NO group (O in black) penetrating the organic layers. (b) View of the structure in the bc plane showing the novel type of κ arrangement of TTF.

Bruker ER200 spectrometer equipped with a helium cryostat. Single-crystal conductivity measurements using the standard four-probe technique were performed on single crystals of a typical size ($0.2 \times 0.2 \times 0.1 \text{ mm}^3$). Platinum wire electrodes ($25 \mu\text{m}$) were attached directly to the most developed face of the crystal (face 100) using graphite paste.

Band Structure Calculations. Both the tight-binding band structure and molecular orbital calculations used an extended Hückel Hamilto-

nian¹² and a modified Wolfsberg–Helmholtz formula¹³ to determine the nondiagonal H_{ij} matrix elements. Double- ζ orbitals¹⁴ for C and S were used. The exponents and parameters used in the calculations were taken from previous work.¹⁵

(12) (a) Whangbo, M.-H.; Hoffmann, R. *J. Am. Chem. Soc.* **1978**, *100*, 6093. (b) Hoffmann, R. *J. Chem. Phys.* **1963**, *39*, 1397.

(13) Ammeter, J.; Bürgi, H.-B.; Thibeault, J.; Hoffmann, R. *J. Am. Chem. Soc.* **1978**, *100*, 3686.

Results and Discussion

Electrochemical oxidation of TTF in the presence of nitroprusside yields the salt $(\text{TTF})_7[\text{Fe}(\text{CN})_5\text{NO}]_2$. The structure consists of layers of TTF and $[\text{Fe}(\text{CN})_5\text{NO}]^{2-}$ complexes alternating along the a axis (Figure 1a). The organic layers are formed by four crystallographically independent TTF molecules, noted as A to D. A remarkable feature in this structure is the unique two-dimensional framework exhibited by the organic part, which is formed by centrosymmetric hexamers of TTF (CBDDBC) and monomers (A) orthogonally packed to form a novel type of κ pattern (Figure 1b). Such a packing contrasts sharply with the marked tendency of TTF to form one-dimensional stackings. To the best of our knowledge, only the series of compounds formulated as $(\text{TTF})_7(\text{MCl}_4)$ ($\text{M} = \text{Co}(\text{II}), \text{Mn}(\text{II}), \text{Zn}(\text{II}), \text{Fe}(\text{III})$) show a similar 2D packing, where the layers are formed by orthogonal TTF trimers.^{16,17} The unprecedented structure of our compound illustrates the considerable effect of the nitroprusside anion on the packing mode of the organic radical. Looking at the intermolecular contacts in the organic layer, one observes that, within the hexamer, the only strong interaction occurs between the internal molecules B and D, where short $\text{S}\cdots\text{S}$ contacts are involved (3.387 Å). Interactions between B and C molecules, as well as between the two central D molecules, are much weaker and do not involve $\text{S}\cdots\text{S}$ interactions. The shortest BC and DD distances are $\text{S}\cdots\text{C} = 3.454$ Å and $\text{C}\cdots\text{C} = 3.558$ Å, respectively. Short contacts between neighboring hexamers, as well as between the hexamer and the monomer, are also observed. Thus, each D molecule belonging to a hexamer has short $\text{S}\cdots\text{S}$ contacts with a side molecule (C) of the neighboring hexamer and with the monomeric molecule (A). The shortest $\text{S}\cdots\text{S}$ distances are 3.372 and 3.360 Å, respectively. The distribution of the four positive charges over the seven TTF molecules can be estimated from the analysis of the bond distances of each individual TTF molecule as described by Umland et al.¹⁸ We find that molecules A and C are neutral, while molecules B and D are completely charged (+1). Accordingly, from an electronic standpoint, this system may be viewed as formed by $(\text{TTF})_2^{2+}$ dimers surrounded by neutral molecules. This point will be confirmed by the band structure calculations.

Focusing on the anionic layer, one observes that it is formed by discrete $[\text{Fe}(\text{CN})_5\text{NO}]^{2-}$ complexes exhibiting pseudotetragonal arrangements. It is worth noting that the NO ligand is not crystallographically disordered over the six coordination positions but is always located parallel to the a axis, pointing toward the neighboring organic layer and even partially penetrating this layer through the holes left by molecules A, C, and D. Interestingly, the CN group in trans to the NO ligand does not penetrate into this layer. This suggests some interaction(s) between the TTF molecules and the NO group, which is surrounded by sulfur atoms from the neutral (A and C) TTF molecules with one short $\text{S}\cdots\text{O}$ contact of 3.36 Å and three contacts of ca. 3.65 Å. In fact, preliminary DSC measurements

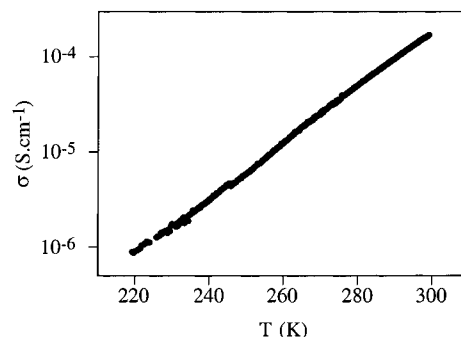


Figure 2. Single-crystal electrical conductivity of $(\text{TTF})_7[\text{Fe}(\text{CN})_5\text{NO}]_2$.

on irradiated polycrystalline samples have shown the existence of a metastable state that decays to the ground state at temperatures as high as 240 K.¹⁹ However, in other irradiated samples of the same compound no decay has been detected. A reason for this may be that only a negligible fraction of nitrosyl complexes are excited because the TTF salt absorbs the exciting light, reducing the penetration depth of the irradiation.

The magnetic properties measured in the temperature range 2–300 K indicate that this salt is diamagnetic. After correction of the susceptibility data for the diamagnetism of the sample and for a weak TIP contribution of $12 \times 10^{-4} \text{ emu}\cdot\text{mol}^{-1}$ from the inorganic component, the magnetic properties show a weak paramagnetic contribution of $\chi T = 0.02 \text{ emu}\cdot\text{K}\cdot\text{mol}^{-1}$, which corresponds to a total amount of paramagnetic impurities of ca. 0.05 spin/mol arising from the organic sublattice. In fact, a very weak and narrow signal (11 G) centered at $g = 2.006$, characteristic of uncoupled TTF^+ radical impurities, is observed in the EPR spectrum at room temperature. Its intensity increases upon cooling, following a Curie law.

The intrinsic diamagnetism of the organic sublattice is consistent with the charge distribution proposed above on the basis of the structure, which suggests that the TTF network is formed by neutral TTF molecules and $(\text{TTF})_2^{2+}$ dimers. Thus, the diamagnetic behavior is merely due to the strong antiferromagnetic coupling between the two spins present in each dimer.

Conductivity measurements indicate that $(\text{TTF})_7[\text{Fe}(\text{CN})_5\text{NO}]_2$ is a semiconductor with a room-temperature conductivity of $4 \times 10^{-4} \text{ S}\cdot\text{cm}^{-1}$ and an activation energy of 420 meV (see Figure 2).

To have a simple description of the electronic structure of this salt (e.g., regarding the extent of charge localization and the chemically significant units of the layer), we carried out both extended Hückel tight-binding band structure calculations for the donor layer and molecular orbital calculations for selected fragments of this layer. According to the structure, the donor slabs of $(\text{TTF})_7[\text{Fe}(\text{CN})_5\text{NO}]_2$ can be described as an orthogonal arrangement of hexameric and monomeric TTF units. Taking into account all $\text{S}\cdots\text{S}$ contacts smaller than 3.9 Å, there are nine different $\text{TTF}\cdots\text{TTF}$ intermolecular interactions in these layers: three intrahexamer interactions, three interhexamer interactions, and three hexamer \cdots monomer interactions. The calculated band structure of the layer is presented in Figure 3. Since the repeat unit of the layer contains 14 TTF molecules, the band structure of Figure 3 contains 14 bands which are mainly built from the HOMO levels of the different donors. Because of the stoichiometry, these HOMO bands must have eight holes. Since there is a relatively large band gap separating

- (14) (a) Whangbo, M.-H.; Williams, J. M.; Leung, P. C. W.; Beno, M. A.; Emge, T. J.; Wang, H. H.; Carlson, K. D.; Crabtree, G. W. *J. Am. Chem. Soc.* **1985**, *107*, 5815. (b) Clementi, E.; Roetti, C. *At. Nucl. Data Tables* **1974**, *14*, 177.
- (15) Pénicaud, A.; Boubekur, K.; Batail, P.; Canadell, E.; Auban-Senzier, P.; Jérôme, D. *J. Am. Chem. Soc.* **1993**, *115*, 4101.
- (16) Maceno, G.; Garrigou-Lagrange, Ch.; Lequan, M.; Lequan, R. M.; Gaultier, J.; Bechtel, F.; Bravic, G.; Delhaes, P. *Synth. Met.* **1988**, *27*, B57.
- (17) Umeya, M.; Kawata, S.; Matsuzaka, H.; Kitagawa, S.; Nishikawa, H.; Kikuchi, K.; Ikemoto, I. *J. Mater. Chem.* **1998**, *8*, 295.
- (18) Umland, T. C.; Allie, S.; Kuhlmann, T.; Coppens, P. *J. Phys. Chem.* **1988**, *92*, 6456.

- (19) Zöllner, H.; Krasser, W.; Woike, Th.; Haussühl, S. *Chem. Phys. Lett.* **1989**, *497*, 161.

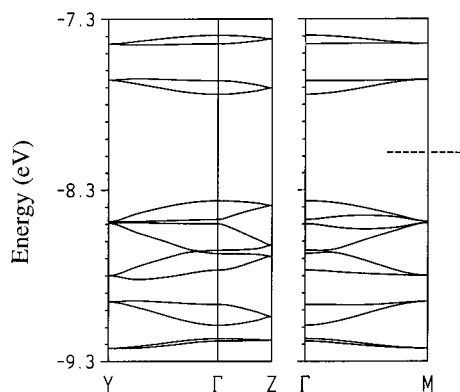


Figure 3. Band structure of the salt $(\text{TTF})_7[\text{Fe}(\text{CN})_5\text{NO}]_2$.

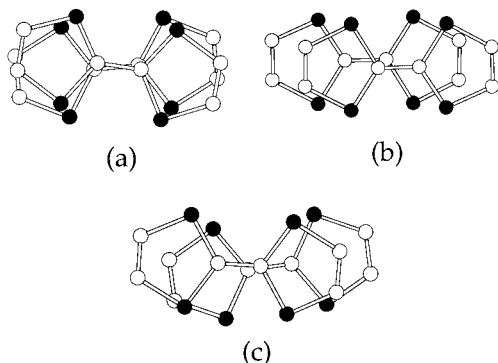


Figure 4. Overlapping modes on the hexameric layers: (a) TTF_B – TTF_D ; (b) TTF_D – TTF_D ; (c) TTF_C – TTF_B .

the four upper bands from the lower ones, we must conclude that these four bands are empty and, thus, we predict an activated conductivity and nonmagnetic properties for $(\text{TTF})_7[\text{Fe}(\text{CN})_5\text{NO}]_2$, in full agreement with the experimental data.

Careful analysis of the upper four bands shows that they are almost exclusively built from the HOMOs of TTFs B and D. The contributions from the HOMOs of the different TTFs to the average composition of the four empty bands are as follows: <1%, TTF A; 53%, TTF B; 5%, TTF C; 40%, TTF D. Thus, it is clear that the monomeric TTF A is a TTF^0 species. It is also clear that the participation of the HOMOs of the outer TTFs of the hexameric unit (TTFs C) in the empty bands, although not completely negligible, is quite small. Thus, TTF C should also be considered as a TTF^0 species. As a consequence, TTFs B and D must be considered as TTF^+ ions. These results are in excellent agreement with an analysis of the bond distances of each individual TTF. Calculations for the tetramer TTF_B – TTF_D – TTF_D – TTF_B and the dimer TTF_B – TTF_D also

show that, of the two possible descriptions of the charge distribution, i.e., two slightly interacting $(\text{TTF}_B$ – $\text{TTF}_D)^{2+}$ dimers and, alternatively, a tetrameric $(\text{TTF}_B$ – TTF_D – TTF_D – $\text{TTF}_B)^{4+}$ unit, the former is more appropriate. The reason for this conclusion is that TTFs B and D adopt a very favorable face to face overlap mode (although slightly rotated; see Figure 4a), leading to very short S···S contacts and, more importantly, to an excellent orientation of the S π orbitals, which result in very strong σ -type overlaps. This leads to a very large S_{HOMO} – HOMO overlap integral and, consequently, to a large splitting between the bonding and antibonding levels. The overlap modes for the TTF_D – TTF_D and TTF_C – TTF_B interactions (see Figure 4b,c) are less favorable in terms of both the S···S intermolecular distances and the orientation of the S π orbitals and lead to S_{HOMO} – HOMO overlap integrals that are approximately half that of the TTF_B – TTF_D interaction. As a consequence, the splitting of the pair of bonding and the pair of antibonding levels of the two identical TTF_B – TTF_D dimers as a result of the TTF_D – TTF_D interaction is small compared with the initial splitting resulting from the strong TTF_B – TTF_D interaction. In addition, the mixing of the HOMO of TTF_C into the high-lying antibonding level of the dimers is small because of both the smaller overlap integral and the bigger energy difference between the two levels. Of course, the three interhexamer interactions and the three monomer···hexamer interactions are much smaller, and thus all bands in Figure 3 are quite flat. In short, the donor layers of $(\text{TTF})_7[\text{Fe}(\text{CN})_5\text{NO}]_2$ can be described as a series of pairs of moderately interacting dimeric $(\text{TTF}_2)^{2+}$ units surrounded by two different types of neutral TTF molecules in such a way that there is no charge delocalization throughout the layer.

More hybrid materials combining other TTF-type organic donors with this and other photochromic nitrosyl complexes are now being investigated by our group to study how the interplay between these two molecular components affects the photo-physical and electrical properties of the final material.

Acknowledgment. This work was supported by the Ministerio de Educación y Cultura (Grant MAT98-0880), by the European Union (TMR Program on Molecular Magnetism), by DGES-Spain Project PB96-0859, and by the Generalitat de Catalunya (Grant 1999 SGR207). M.C.-L. and J.R.G.-M. thank the Generalitat de Valenciana for a predoctoral fellowship.

Supporting Information Available: An X-ray crystallographic file, in CIF format, for $(\text{TTF})_7[\text{Fe}(\text{CN})_5\text{NO}]_2$. This material is available free of charge via the Internet at <http://pubs.acs.org>.

IC0002566